

Imaging of HER3-expressing xenografts in mice using a $^{99m}\text{Tc}(\text{CO})_3\text{-HEHEHE-Z}_{\text{HER3:08699}}$ affibody molecule

Anna Orlova · Magdalena Malm · Maria Rosestedt · Zohreh Varasteh · Ken Andersson · Ram Kumar Selvaraju · Mohamed Altai · Hadis Honarvar · Joanna Strand · Stefan Ståhl · Vladimir Tolmachev · John Löfblom

Received: 6 October 2013 / Accepted: 17 February 2014 / Published online: 13 March 2014
© Springer-Verlag Berlin Heidelberg 2014

Abstract

Purpose Human epidermal growth factor receptor type 3 (HER3) is a transmembrane receptor tyrosine kinase belonging to the HER (ErbB) receptor family. Membranous expression of HER3 is associated with trastuzumab resistance in breast cancer and the transition to androgen independence in prostate cancer. Imaging of HER3 expression in malignant tumors may provide important diagnostic information that can influence patient management. Affibody molecules with low picomolar affinity to HER3 were recently selected. The aim of this study was to investigate the feasibility of HER3 imaging using radiolabeled Affibody molecules.

Methods A HER3-binding Affibody molecule, Z_{08699} , with a HEHEHE-tag on N-terminus was labeled with $^{99m}\text{Tc}(\text{CO})_3$ using an IsoLink kit. In vitro and in vivo binding specificity and the cellular processing of the labeled binder were evaluated. Biodistribution of $^{99m}\text{Tc}(\text{CO})_3\text{-HEHEHE-Z}_{08699}$ was studied over time in mice bearing HER3-expressing xenografts.

Results HEHEHE- Z_{08699} was labeled with $^{99m}\text{Tc}(\text{CO})_3$ with an isolated yield of >80 % and a purity of >99 %. Binding of $^{99m}\text{Tc}(\text{CO})_3\text{-HEHEHE-Z}_{08699}$ was specific to BT474 and MCF7 (breast cancer), and LS174T (colon cancer) cells.

Cellular processing showed rapid binding and relatively quick internalization of the receptor/Affibody molecule complex (70 % of cell-associated radioactivity was internalized after 24 h). The tumor targeting was receptor mediated and the excretion was predominantly renal. Receptor-mediated uptake was also found in the liver, lung, stomach, intestine, and salivary glands. At 4 h pi, tumor-to-blood ratios were 7 ± 3 for BT474, and 6 ± 2 for LS174T xenografts. LS174T tumors were visualized by microSPECT 4 h pi.

Conclusions The results of this study suggest the feasibility of HER3-imaging in malignant tumors using Affibody molecules.

Keywords HER3 · Affibody molecule · Technetium-99 m · Molecular imaging · Molecular targeting

Introduction

Human epidermal growth factor receptor type 3 (HER3, in non-human ErbB3) is a member of the HER family of receptor tyrosine kinases (RTK). This family is called HER (in humans) or the type I RTK family [1, 2]. For the majority of these receptors, binding of a ligand causes conformational changes that facilitate homo- and heterodimerization followed by activation of the intracellular tyrosine kinase domains. Downstream signaling of HER-receptors is involved in the regulation of cell proliferation, differentiation, motility, and apoptosis. It has also been shown that the deregulation of HER family expression and signaling is associated with malignant transformation and tumor progression [2]. Interestingly, the intracellular domain of HER3 lacks full kinase activity, and signaling through HER3 occurs by heterodimerization with other members of the HER family [1].

Targeting of aberrantly expressed receptors from the HER family using monoclonal antibodies, antibody-drug

Electronic supplementary material The online version of this article (doi:10.1007/s00259-014-2733-7) contains supplementary material, which is available to authorized users.

A. Orlova (✉) · M. Rosestedt · Z. Varasteh · R. K. Selvaraju
Preclinical PET Platform, Department of Medicinal Chemistry,
Uppsala University, Uppsala, Sweden
e-mail: anna.orlova@pet.medchem.uu.se

M. Malm · K. Andersson · S. Ståhl · J. Löfblom
Division of Protein Technology, School of Biotechnology, KTH
Royal Institute of Technology, Stockholm, Sweden

M. Altai · H. Honarvar · J. Strand · V. Tolmachev
Division of Biomedical Radiation Sciences, Rudbeck Laboratory,
Uppsala University, Uppsala, Sweden

conjugates, and tyrosine kinase inhibitors are the most promising approaches for the treatment of disseminating cancer [3]. Until recently, the main focus has been on targeting HER1 (EGFR) and HER2 [4]. However, a growing amount of evidence suggests that HER3 expression is a cause of resistance to HER1- and HER2-targeted therapies and to chemotherapy [5–9]. Moreover, there are indications that HER3 expression is associated with the transition of prostate cancer to castration resistance [10]. Consequently, in 2012, six HER3-targeting monoclonal antibodies or antibody-based constructs were in clinical trials, and six more were in preclinical development [4]. However, only a fraction (17–60 %, depending on origin) of tumors overexpress HER3 [11], which necessitates the development of companion diagnostics permitting determination of HER3 expression status to select patients who would most likely respond to HER3-targeting therapy.

Currently, molecular profiling of tumors is mainly performed on biopsy samples. However, biopsies are invasive and cannot be frequently repeated. The predictive power is also limited by the risk of non-representative samplings due to intratumoral expression heterogeneity. The target expression levels might also vary during the course of therapy. Radionuclide molecular imaging of therapeutic targets has the potential to successfully challenge the current practice in patient stratification for specific therapies [12, 13]. Imaging-based methods are non-invasive and allow for serial investigations, which is essential for pharmacodynamic studies. Moreover, sampling errors due to expression heterogeneities are reduced.

A common approach for the molecular imaging of therapeutic targets is the use of radiolabeled antibodies [14]. Currently, a radiolabeled anti-HER3 antibody U3-1287 is in clinical trials (NCT01479023). However, intact antibodies are suboptimal imaging agents. Their large size (150 kDa) causes slow extravasation as well as poor tumor penetration, and the clearance of antibodies from blood is slow, resulting in a high background activity. Imaging using intact antibodies is thus typically associated with low contrast and sensitivity. Moreover, antibodies, as with other proteins having a molecular weight of more than 45 kDa, accumulate in tumors unspecifically due to the “enhanced permeability and retention” (EPR) effect [15], which is associated with a risk of false-positive findings. The use of smaller imaging agents should improve both the sensitivity and specificity of molecular imaging.

Affibody molecules are small (7 kDa) three-helical scaffold proteins originally derived from the B-domain of staphylococcal protein A. By randomization of 13 surface-exposed residues, diverse molecular libraries have been generated from which high-affinity binders have been selected by various display techniques [16]. Until today, a number of Affibody molecules with subnanomolar affinities to cancer-associated molecular targets such as HER2 [17], HER1 [18], and IGF-1R

[19] have been developed and evaluated as imaging agents. Their small size facilitates rapid extravasation and tumor penetration, as well as the rapid clearance of unbound tracers. Together with very high affinity, this permits high-contrast imaging of target expression within a few hours after injection. Multiple studies with different xenograft models have demonstrated that there is no unspecific uptake of Affibody molecules in tumors, which is important in order to exclude false-positive findings [20–22]. Two clinical studies have confirmed the potential of Affibody-based agents for the imaging of HER2-expressing metastases in patients with disseminated breast cancer [23, 24]. The positive results encouraged us to develop HER3-binding Affibody molecules that may be used for the imaging of HER3 expression *in vivo*.

A first selection of HER3-binding Affibody molecules resulted in the isolation of specific binders with affinities around 1 nM to both human HER3 and murine ErbB3 [25]. One of the challenges of imaging HER3 is the modest overexpression, typically below 50,000 receptors per cell [26]. Our experience from HER2-targeting Affibody molecules is that imaging of such expression levels requires low picomolar affinity [22]. To meet these requirements, additional affinity maturation was performed using bacterial display [27] and fluorescence-activated cell sorting (FACS), resulting in the selection of the Z₀₈₆₉₈ and Z₀₈₆₉₉ Affibody molecules with affinities of around 50 and 21 pM, respectively [28]. Specificity of new Affibody molecules to HER3 was demonstrated by FACS and surface plasmon resonance (SPR) (both against HER3-Fc), and through inhibition experiments (against heregulin on MCF7 cells).

In this study, we tested the feasibility of imaging HER3-expressing xenografts *in vivo* using a radiolabeled Z₀₈₆₉₉ Affibody molecule. To facilitate labeling using Tc-tricarbonyl chemistry, a histidyl-glytamyl-histidyl-glytamyl-histidyl-glytamyl- (HEHEHE)-tag was engineered at the N-terminus of Z₀₈₆₉₉, as this tag permits an immobilized metal ion affinity chromatography (IMAC) purification of Affibody molecules and provides improved biodistribution properties [29, 30]. Biochemical and biophysical properties of the novel construct were characterized, and targeting of HER3-expressing cells using ^{99m}Tc(CO)₃-HEHEHE-Z₀₈₆₉₉ was evaluated *in vitro* and *in vivo*.

Materials and methods

Materials

Radioactivity was measured using an automated gamma-counter with a 3-inch NaI(Tl) detector (1480 WIZARD, Wallac Oy). The purity of radiolabeled Affibody molecules was determined by radio-ITLC (150–771 DARK GREEN, Tec-Control Chromatography strips from Biodex Medical

Systems) and cross-validated by sodium dodecyl sulfate polyacrylamide gel electrophoresis (SDS PAGE) and size exclusion chromatography. The distribution of radioactivity along instant thin-layer chromatography (ITLC) strips and SDS gels was measured on a Cyclone™ Storage Phosphor System and analyzed using the OptiQuant™ image analysis software (PerkinElmer). All animal experiments were planned and performed in accordance with national legislation on the protection of laboratory animals and were approved by the Ethics Committee for Animal Research in Uppsala.

Data were assessed by an unpaired, two-tailed *t*-test using GraphPad Prism (version 4.00 for Windows GraphPad Software) in order to determine significant differences ($p < 0.05$).

Expression, purification, and characterization of HEHEHE- Z_{08699}

Subcloning, protein production, purification and characterization of HEHEHE- Z_{08699} was essentially performed as previously described [28]. Details of subcloning, protein production, purification, and characterization of HEHEHE- Z_{08699} are described in [Online Resource](#).

Labeling of HEHEHE- Z_{08699} with [$^{99m}\text{Tc}(\text{CO})_3$] $^+$ and analysis of labeling stability

Labeling of HEHEHE- Z_{08699} with [$^{99m}\text{Tc}(\text{CO})_3$] $^+$ was performed as described by Tolmachev and co-workers [27]. For labeling 500 μl of $^{99m}\text{TcO}_4^-$ -containing generator eluate was added to a vial with the IsoLink kit. The mixture was incubated at 100 °C for 20 min. Thereafter, 40 μl of mixture (200–320 MBq) was transferred to a tube containing 50 μg (~6.8 nmol) Affibody molecules in 40 μl PBS and incubated at 50 °C for 60 min. Labeling of Z_{08699} -His₆ was done as described in Malm et al [26]. The labeling yield was measured by ITLC. When the ITLC strips are eluted with PBS, pertechnetate, as well as carbonyl and histidine complexes of ^{99m}Tc migrate with the eluent front ($R_f=1.0$), while Affibody molecules do not migrate under these conditions ($R_f=0.0$). To determine the presence of reduced hydrolyzed technetium, ITLC was eluted with pyridine:acetic acid:water (5:3:1.5). When this eluent is used, the technetium colloids stay at the application point ($R_f=0.0$), while the radiolabeled Affibody molecule, as well as pertechnetate and carbonyl complexes of ^{99m}Tc migrate with the solvent front ($R_f=1.0$). In addition, blank experiments were performed, where the Affibody molecule was omitted. The labeled Affibody molecule was purified using NAP-5 desalting columns, pre-equilibrated and eluted with PBS. The purity of each preparation was evaluated using ITLC. Radio-ITLC was cross-validated by SDS-PAGE and size-exclusion chromatography as described in [Online Resource](#).

To determine shelf-life of the conjugates, $^{99m}\text{Tc}(\text{CO})_3$ -HEHEHE- Z_{08699} and $^{99m}\text{Tc}(\text{CO})_3$ - Z_{08699} -His₆ were incubated in PBS at RT. To evaluate the stability of the ^{99m}Tc -label, a histidine challenge of the conjugates was performed [31]. Samples were incubated at 37 °C with 500- and 5,000-fold excess of histidine during 4 h. The samples were analyzed using ITLC. To determine the stability of $^{99m}\text{Tc}(\text{CO})_3$ -HEHEHE- Z_{08699} in blood, 50 μl of freshly labeled conjugate were incubated with 300 μl of human blood plasma for 1 h at 37 °C, and the mixture was analyzed by SDS-PAGE and size-exclusion chromatography as described in [Online Resource](#).

In-vitro cell binding, and cellular processing of $^{99m}\text{Tc}(\text{CO})_3$ -HEHEHE- Z_{08699}

Cells with documented expression of HER3, a colorectal carcinoma LS174T [32], and breast cancer BT474 [33] and MCF-7 [34] cell lines, were used to study the specificity of $^{99m}\text{Tc}(\text{CO})_3$ -HEHEHE- Z_{08699} for binding in vitro. All cell lines were from American Type Tissue Culture Collection. Receptor expression was estimated for each used cell line. A measurement of the rate of internalization of $^{99m}\text{Tc}(\text{CO})_3$ -HEHEHE- Z_{08699} was performed for BT474 and LS174T cells. An in-vitro specificity test and cellular processing study was performed in triplicate according to methods described earlier [35].

To study the specificity of binding in vitro, a solution of radiolabeled Affibody molecules (0.2 nM) was added to the cells in plates. For blocking, 0.2 μM of non-labeled Affibody molecule was added 15 min before radiolabeled conjugates to saturate the receptors. The cells were incubated for 2 h at room temperature to prevent internalization. Thereafter, the media was collected, the cells were detached using trypsin-EDTA solution (0.25 % trypsin, 0.02 % EDTA in buffer, Biochrom AG, Berlin, Germany) and re-suspended, and the radioactivity in cells and media was measured to enable calculation of the fraction of cell-bound radioactivity. A small fraction of the cell suspension was used for cell counting.

To study cellular processing, the cells were incubated with the labeled compound (0.2 nM) at 37 °C. At pre-determined time points, the medium from a set of three dishes was removed. To collect the membrane-bound radioactivity, the cells were treated with 0.2 M glycine buffer containing 4 M urea, pH 2.5, for 5 min on ice. To collect the radioactivity internalized by the cells, treatment with 1 M NaOH at 37 °C for 0.5 h was performed. The percentage of internalized radioactivity was calculated for each time point.

Biodistribution studies

Two groups of NMRI mice ($n=4$) were intravenously (iv) injected with $^{99m}\text{Tc}(\text{CO})_3$ -HEHEHE- Z_{08699} or $^{99m}\text{Tc}(\text{CO})_3$ -

Z₀₈₆₉₉-His₆ (1 µg/100 µl PBS) with the aim of comparing their biodistribution. The animals were sacrificed at 4 h pi by injection of a lethal dose of anesthesia (20 µl of Ketalar-Rompun per gram body weight: Ketalar (50 mg/ml, Pfizer), 10 mg/ml; Rompun, (20 mg/ml, Bayer) followed by heart puncture and exsanguination with a heparinized syringe. Samples of blood and organs were collected and their radioactivity was measured. Tissue uptake was calculated as the percentage of injected radioactivity per gram (%ID/g). Radioactivity in the carcass and gastrointestinal tract was calculated as %ID per whole sample.

To evaluate the targeting of HER3-expressing tumors *in vivo*, mice bearing LS174T and BT474 xenografts were used. LS174T cells (10⁶ cells) were implanted subcutaneously in female Balb/c nu/nu mice 2 weeks before the experiment. BT474 cells (10⁷ cells) were implanted in 50 % Matrigel in female Balb/c nu/nu mice pre-implanted with estradiol pellets (0.5 mg/d, 21 days; Innovative Research of America) 3 weeks before the experiment. Mice with LS174T xenografts received intravenous injections of 1 µg of ^{99m}Tc(CO)₃-HEHEHE-Z₀₈₆₉₉, and radioactivity distribution was studied at 1, 4 and 8 h pi (*n*=4) as described above.

In an additional experiment to evaluate if the uptake in tumors and mErbB3-expressing organs was saturable, ^{99m}Tc(CO)₃-HEHEHE-Z₀₈₆₉₉ was intravenously injected in two group of mice (*n*=4). The injected protein dose was adjusted by dilution with non-labeled affibody molecules to 1 (0.13 nmol) or 70 µg (9 nmol) per mouse. The animals were sacrificed at 4 h pi as described above. Biodistribution was measured as described above.

Imaging studies

The imaging was performed to obtain a visual confirmation of the biodistribution results. An LS174T tumor-bearing mouse was injected with ^{99m}Tc(CO)₃-HEHEHE-Z₀₈₆₉₉ (1.6 MBq/1 µg). Four hours pi, the animal was euthanized and the urinary bladder was excised post-mortem to improve image quality. A static whole-body tomographical examination was then performed in the Triumph™ Trimodality System (TriFoil Imaging, Inc.). A SPECT scan was performed with parameters (FOV: 8 cm, 75A10 collimators, acquisition over 200–250 keV, 32 projections) and SPECT raw data was reconstructed by FLEX SPECT software using an ordered Subset Expectation Maximization (OSEM) iterative reconstruction algorithm. The CT raw files were reconstructed using Filter Back Projection (FBP).

SPECT and CT dicom files were fused and analyzed using PMOD v3.12 (PMOD Technologies Ltd). The color scale of coronal images was expressed as %ID/g.

Results

Expression and purification of HEHEHE-Z₀₈₆₉₉

The Affibody molecule, HEHEHE-Z₀₈₆₉₉, was produced in *E. coli* under control of the T7 promoter. The results from the mass spectroscopy analysis verified that the molecular weight of the purified protein was in accordance with the theoretical mass (7582 Da vs. 7583 Da) and the analytical reverse phase high-performance liquid chromatography (RP-HPLC) demonstrated a purity of >99 %. Surface plasmon resonance analysis confirmed retained affinity of the Affibody molecule for HER3 and mErbB3 (Table 1). The melting point was 66 °C. Circular dichroism spectroscopy demonstrated that HEHEHE-Z₀₈₆₉₉ had a helical content that is typical for correctly folded three-helical bundle Affibody molecules, and demonstrated identical helical content before and after heat treatment, indicating complete refolding after thermal denaturation.

Labeling of HEHEHE-Z₀₈₆₉₉ and stability of the product

The average radiochemical yield for ^{99m}Tc(CO)₃-HEHEHE-Z₀₈₆₉₉ was 94±7 %, the isolated yield was 82±4 %; the radiochemical purity after size-exclusion purification (disposable NAP-5 column) was 99.2±0.8 % with a maximum specific radioactivity of 1.6 MBq/µg (12 MBq/nmol). The labeling yield for ^{99m}Tc(CO)₃-Z₀₈₆₉₉-His₆ was 91 % and the purity after NAP-5 purification was 99.7 %, as shown in Online Resource (Figs. S1 and S2).

The results of shelf-life and stability tests are presented in Table 2. There was no detectable release of ^{99m}Tc after storage of the conjugate, indicating that the shelf-life of ^{99m}Tc(CO)₃-HEHEHE-Z₀₈₆₉₉ is at least 4 h. The conjugate was stable under histidine challenge and incubation in blood plasma (later data are not shown). Both conditions demonstrated no release of activity from ^{99m}Tc(CO)₃-HEHEHE-Z₀₈₆₉₉ as compared with the control. Similar stability was found for ^{99m}Tc(CO)₃-Z₀₈₆₉₉-His₆.

In-vitro specificity and cellular processing, B_{max} estimation

All tested cell lines bound to the anti-HER3 Affibody molecule, specifically because the saturation of the receptors by

Table 1 Surface plasmon resonance data for HEHEHE-Z₀₈₆₉₉ Affibody molecule

	k _a (1/Ms)	k _d (1/s)	K _D (M)
hHER3	2.93*10 ⁶	8.50*10 ⁻⁵	2.27*10 ⁻¹¹
mErbB3	3.32*10 ⁶	1.74*10 ⁻⁴	5.26*10 ⁻¹¹

Table 2 In-vitro stability of [$^{99m}\text{Tc}(\text{CO})_3$] $^+$ -labeled Affibody molecules. Incubation in PBS at room temperature (RT) was performed to determine shelf-life. The challenge was performed by incubation with an excess of histidine at 37 °C for 4 h. The data are presented as an average % radioactivity associated with Affibody molecule of the two experiments with maximum error

	HEHEHE- Z_{08699}	Z_{08699} -His $_6$
PBS	99.7±0.0	99.5±0.1
500-fold excess of histidine	99.55±0.05	98.4±0.1
5,000-fold excess of histidine	99.0±0.2	97.05±0.05

pre-incubation with non-labeled Affibody molecules significantly ($p<0.05$) decreased the binding of the radiolabeled one (Fig. 1). The estimated receptor density was $8\pm 1\times 10^3$ receptors/cell for LS174T, $13\pm 3\times 10^3$ for MCF7, and $25\pm 2\times 10^3$ for BT474 cells.

The pattern of cellular uptake of $^{99m}\text{Tc}(\text{CO})_3$ -HEHEHE- Z_{08699} at continuous incubation differed between the BT474 and LS174T cell lines, but the rate of internalization was similar (Fig. 2). Cell-associated radioactivity continuously increased for LS174T cells and reached 23 % from added radioactivity at 24 h. For BT474 cells, maximum cell bound radioactivity was reached at 8 h of continuous incubation followed by plateau. Internalization of radioactivity was rapid: at 4 h of incubation, it was up to 50 % of the total cell-associated radioactivity. After 24 h continuous incubation, 65–70 % of cell-associated radioactivity was internalized.

In vivo studies

Biodistribution of $^{99m}\text{Tc}(\text{CO})_3$ -HEHEHE- Z_{08699} and $^{99m}\text{Tc}(\text{CO})_3$ - Z_{08699} -His $_6$ was studied in NMRI female mice at 4 h post i.v. injection of 1 μg of protein (Fig. 3). Radioactivity concentration was significantly lower for $^{99m}\text{Tc}(\text{CO})_3$ -HEHEHE- Z_{08699} in all studied tissues than that for $^{99m}\text{Tc}(\text{CO})_3$ - Z_{08699} -His $_6$, except in the kidneys and gastro-

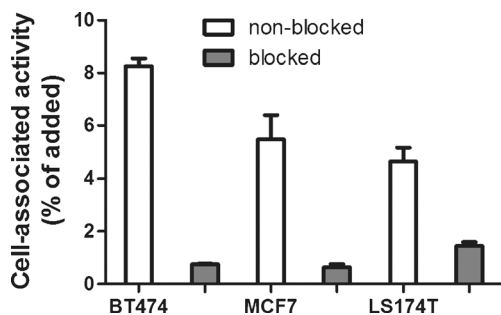


Fig. 1 Specific binding of $^{99m}\text{Tc}(\text{CO})_3$ -HEHEHE- Z_{08699} to HER3-expressing carcinoma cell lines. For the pre-saturation of HER3, a 1,000-fold molar excess of non-radioactive HEHEHE- Z_{08699} Affibody molecule was added. Data are presented as mean values from three samples \pm SD

intestinal tract (with content). Radioactivity concentration decreased more than 2-fold in a majority of the studied organs and more than 3-fold in the liver and bones.

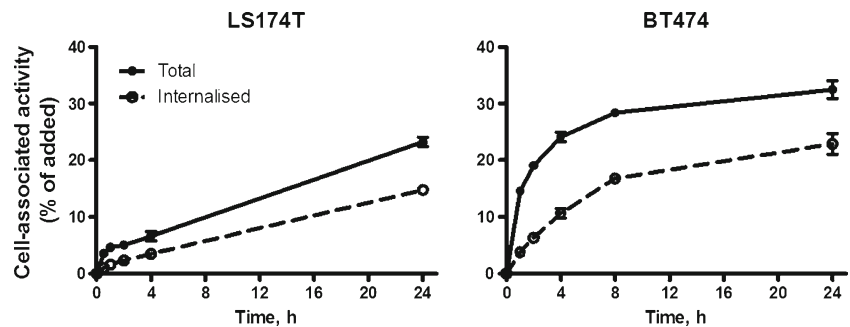
Data for the biodistribution of $^{99m}\text{Tc}(\text{CO})_3$ -HEHEHE- Z_{08699} in mice bearing LS174T xenografts over time are presented in Fig. 4. Blood clearance was fast, with the remaining 1 %ID/g already at 1 h pi followed by further decrease. This rapid clearance translated to low radioactivity concentration in muscle and bones. Tumor uptake of radioactivity was ~ 4 %ID/g at 1 h pi, but decreased two-fold to 4 h pi and then remained stable. In accordance with data for NMRI mice, the predominant excretion pathway was renal, with a slow release of absorbed radioactivity over time. Uptake of radioactivity in mErbB3-expressing organs was high, but appreciable wash-out was found in the salivary glands, lungs, liver, and organs of the gastrointestinal tract. Ratios of tumor-to-blood and to the majority of organs increased with time. Tumor-to-blood ratio was 3.9 ± 0.5 already at 1 h pi and reached 9.1 ± 0.7 at 8 h pi. Tumor-to-muscle increased from 16 at 1 h pi to 19 at 8 h, and tumor-to-bone was around 7 at all times of observation. The only organ for which the tumor-to-non-tumor ratio decreased with time was spleen. In the liver and small intestine, the radioactivity concentration was higher than that in tumors at all investigated time points.

$^{99m}\text{Tc}(\text{CO})_3$ -HEHEHE- Z_{08699} demonstrated specific binding to HER3 in LS174T and BT474 xenografts, as well as to murine ErbB3. The radioactivity concentration was significantly decreased in all studied organs and tissues, except in bones for both models and in the spleen for BT474, when the injected protein dose was increased from 1 to 70 $\mu\text{g}/\text{mouse}$ (Fig. 5). Radioactivity concentration in the kidneys was, on the contrary, increased with a higher injected protein dose (for BT474 mice significantly). Radioactivity cleared rapidly from blood, muscle, and bones. Radioactivity was predominantly excreted via the kidneys with a high degree of renal re-absorption. Liver uptake was receptor-mediated and was on the level of 3–6%ID/g. Tumor uptake was $1.7\pm 0.6\%$ ID/g for BT474 and $2.2\pm 0.3\%$ ID/g for LS174T xenografts. Tumor uptake was lower than uptake in the liver and small intestine for both tested models. Tumor-to-non-tumor ratios were similar for both models and tumor-to-blood ratios were 7 ± 3 for BT474 and 6 ± 2 for LS174T xenografts. Tumor-to-bone ratios were 10 ± 4 for BT474 and 7 ± 1 for LS174T xenografts, and tumor-to-muscle ratios were 11–12 for both xenograft models.

For convenience, all tabulated data for in vivo experiments are given in [Online Resource](#).

Image acquired 4 h after administration of $^{99m}\text{Tc}(\text{CO})_3$ -HEHEHE- Z_{08699} to an immunodeficient mouse bearing a subcutaneous LS174T xenograft is presented in Fig. 6. The highest radioactivity was observed in the kidney (Fig. 6a), which exceeded uptake in any other organ or tissue. Setting

Fig. 2 Binding and internalization of $^{99m}\text{Tc}(\text{CO})_3\text{-HEHEHE-Z}_{08699}$ by LS174T (colorectal carcinoma) and BT474 (breast carcinoma) cell lines. Cells were incubated with 0.2 nM $^{99m}\text{Tc}(\text{CO})_3\text{-HEHEHE-Z}_{08698}$ at 37 °C. Data are presented as mean values from three samples \pm SD



the upper threshold at 3%ID/g permitted visualization of liver. The tumor was also clearly visualized in these settings (Fig. 6b).

Discussion

The current development of HER3-targeting therapeutic antibodies has put forward a requirement for the identification of patients who would benefit from such therapy. However, there are challenges associated with the development of probes for HER3 visualization. One challenge is the relatively abundant expression of HER3 in normal organs and tissues, such as liver, stomach, small intestines, salivary glands, and lung (<http://www.proteinatlas.org>). Receptors in normal tissues thus might efficiently sequester an imaging probe from the circulation. Particularly challenging is the presence of HER3 in liver, as this organ is very well perfused, and the liver vasculature is well-fenestrated. Thus, there is a risk that an imaging probe would be trapped in the liver without reaching the tumor. Yet, we have previously demonstrated that the optimization of an injected protein dose might permit us to find a dose allowing sufficient saturation of receptors in the liver without saturating tumors (as exemplified by targeting HER1 [18]). Imaging of HER3 is, however, even more challenging, as it is generally also expressed at a relatively low level in tumors. Previous experiments [36] have shown that

exceeding an injection dose of 1 μg (0.13 nmol) per mouse causes an appreciable reduction of uptake in tumors expressing 40,000 HER2/cell, i.e., having the same expression level range as HER3-expressing cell lines. This was also observed when the imaging properties of anti-IGF1R Affibody molecules were evaluated in a murine model [19]. IGF1R expression in the used xenograft model was on the same level as typically seen for HER3, the anti-IGF1R Affibody molecule also had cross-reactivity to murine IGF1R, and the presence of IGF1R expression in normal tissues had the same pattern as in this study. In this circumstance, the cross-reactivity of an imaging agent with murine ErbB3 is important in order for the xenograft model in mice to be relevant. The Affibody molecule Z_{08699} studied in this paper met this criterion.

Technetium-99 m is still the most widely used nuclide for clinical imaging due to its favorable emission profile, good availability, and low cost due to generator production and wide availability of SPECT/CT scanner in clinics. The use of $^{99m}\text{Tc}(\text{CO})_3(\text{H}_2\text{O})_3$ -mediated chemistry [37] permits a facile site-specific labeling of histidine-containing recombinant proteins using a simple two-vial kit. Initial experiments on the labeling of HER3-targeting Affibody molecules have been performed using variants containing hexahistidine tags at the C-terminus [28], as such placement provides more favorable biodistribution than N-terminal placement [29]. However, our recent findings suggest that placement of a histidyl-glytanyl-histidyl-glytanyl-(HEHEHE)-tag at the N-terminus provides the best biodistribution profile of $^{99m}\text{Tc}(\text{CO})_3$ -labeled Affibody molecules [30]. Accordingly, $\text{Z}_{08699}\text{-His}_6$ was therefore re-engineered to HEHEHE- Z_{08699} .

Labeling of HEHEHE- Z_{08699} with $^{99m}\text{Tc}(\text{CO})_3$ using a commercially available IsoLink kit provided a high, isolated yield of over 80 % using size-exclusion column, and with radiochemical purity of over 99 %. $^{99m}\text{Tc}(\text{CO})_3\text{-HEHEHE-Z}_{08699}$ was stable both in PBS during 4 h and under histidine challenge. Binding specificity of $^{99m}\text{Tc}(\text{CO})_3\text{-HEHEHE-Z}_{08699}$ to HER3-expressing cells was preserved. The selected panel of cell-lines demonstrated expression levels in the range of 8–25,000 receptors per cells. A cellular processing study

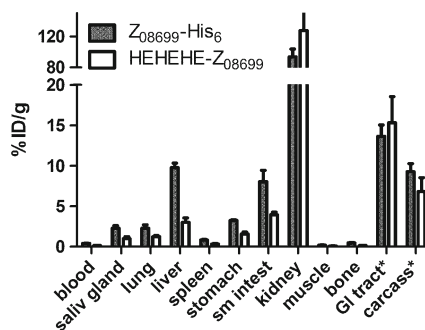
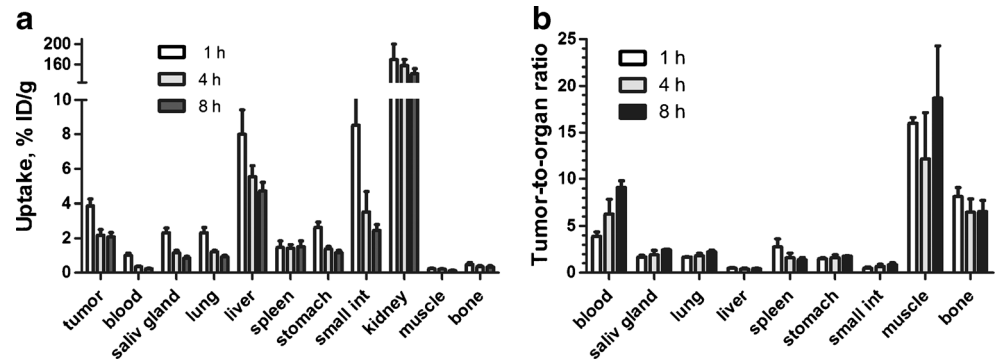


Fig. 3 Biodistribution 4 h pi of 1 μg of $^{99m}\text{Tc}(\text{CO})_3\text{-HEHEHE-Z}_{08699}$ or $^{99m}\text{Tc}(\text{CO})_3\text{-Z}_{08699}\text{-His}_6$ in female NMRI mice. Values are presented as mean %ID/g and error-bars correspond to SD ($n=4$)

Fig. 4 A. Biodistribution of 1 μg of $^{99\text{m}}\text{Tc}(\text{CO})_3\text{-HEHEHE-Z}_{08699}$ in female Balb/c nu/nu mice with LS174T subcutaneous xenografts. B. Tumor-to-non-tumor ratios. Values are presented as mean and error-bars correspond to SD ($n=4$)



revealed an interesting feature of the HER3-binding Affibody molecule, which is a relatively rapid internalization rate of the receptor-ligand complex. After a 4-h incubation, up to half of the radioactivity was internalized. For comparison, the internalization of an HER2-targeting Affibody molecules is only 10–15 % at this time [35]. The moderately residualizing properties of $^{99\text{m}}\text{Tc}(\text{CO})_3\text{-HEHEHE}$ [29] would be suitable for the labeling of a targeting protein with an elevated internalization rate. However, the use of a label with stronger residualizing properties, e.g., ^{111}In , in combination with macrocyclic chelators might offer further improvement of intracellular retention of radioactivity associates with internalized conjugate.

The in vivo comparison of the biodistribution of new (HEHEHE-tagged) and old (His-tagged) constructs confirmed our previous observations [29, 30] that more hydrophilic HEHEHE-tag improves the biodistribution pattern of the Affibody molecule (Fig. 3). Particularly the use of HEHEHE-tag at the N-terminus provided an appreciable reduction of hepatic uptake in comparison with a previous variant, which was labeled via a hexahistidine tag at C-terminus [28]. Liver uptake of $^{99\text{m}}\text{Tc}(\text{CO})_3\text{-HEHEHE-Z}_{08699}$ was 3.0 ± 0.5 %ID/g, while the uptake of $^{99\text{m}}\text{Tc}(\text{CO})_3\text{-Z}_{08698}\text{-H}_6$ was 9.8 ± 0.6 %ID/g. A two-fold decrease in radioactivity uptake was found in the majority of the studied organs despite the same affinity to mErbB3 for both constructs.

The tumor uptake was higher than uptake in other organs and tissues, except from the kidneys, liver and small intestine wall when the biodistribution of conjugate was studied in xenografted mice (Figs. 4 and 5). The high renal re-absorption of the radioactivity was similar to re-absorption of Affibody molecules to other tyrosine kinase receptors (e.g. HER2 [38], HER1 [18], IGF-1R [19], PDGFR β [39]), and is, probably, a property of this scaffold. Radioactivity accumulation in the kidneys was not reduced with time, which reflected the residualizing properties of the label and was in agreement with previous observations for small proteins labeled using $^{99\text{m}}\text{Tc}(\text{CO})_3$ [37, 40]. Hepatocytes and bile duct cells in liver and glandular cells in intestine walls have medium HER3 expression (<http://www.proteinatlas.org>). Taking into account that the in vivo specificity study demonstrated that radioactivity uptake in these organs was saturable, we can conclude that this uptake was receptor specific. Previously, an Affibody molecule with an unrelated specificity for Taq polymerase (Z_{Taq}), which has the same 3-helix structure and that only differs in the few amino acids in the binding region, was tested for biodistribution and tumor uptake in the LS174T xenograft model [20, 22]. The level of radioactivity concentration in tumors due to unspecific uptake was lower or on the level of muscles and blood. Radioactivity levels decreased constantly in normal mErbB3-expressing organs over time, while remaining constant in tumors between 4 and 8 h pi,

Fig. 5 Biodistribution 4 h pi of 1 and 70 μg of $^{99\text{m}}\text{Tc}(\text{CO})_3\text{-HEHEHE-Z}_{08699}$ in female Balb/c nu/nu mice with subcutaneous xenografts. Values are presented as mean %ID/g and error-bars correspond to SD ($n=4$)

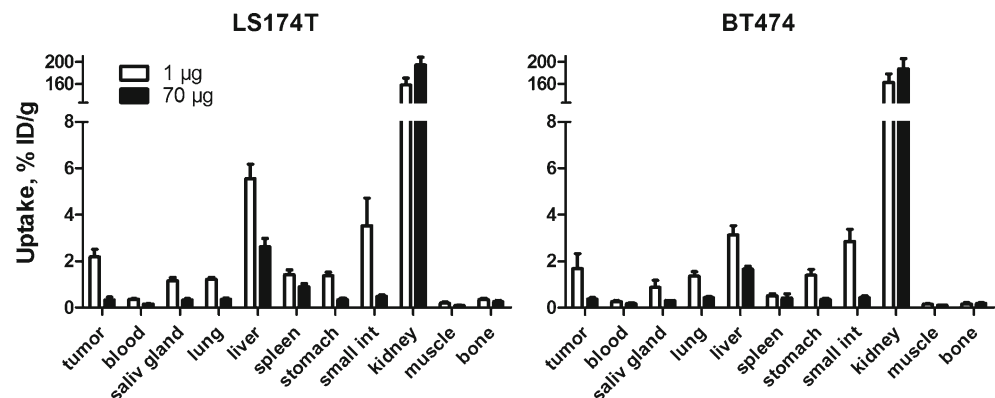
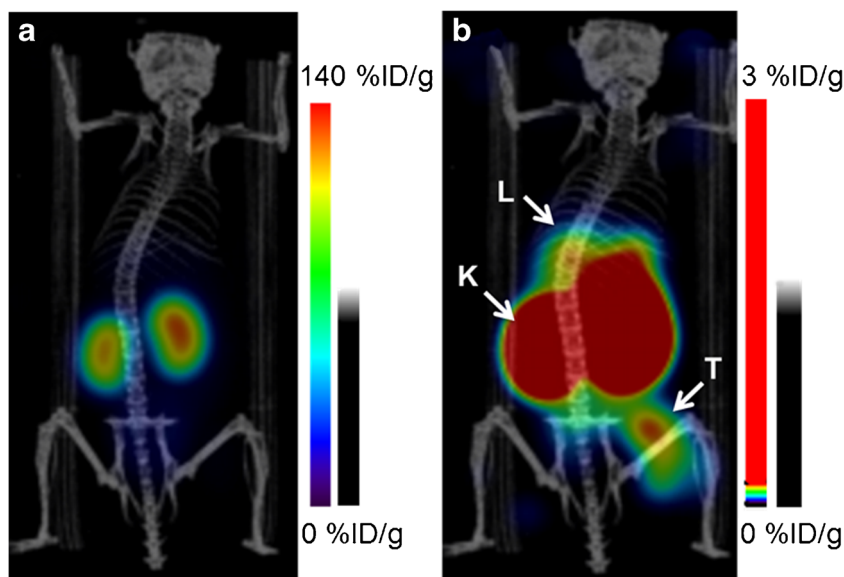


Fig. 6 Imaging of HER3 expression, 4 h pi, in LS174T colorectal carcinoma xenografts in Balb/c nu/nu mouse using $^{99m}\text{Tc}(\text{CO})_3\text{-HEHEHE-Z}_{08699}$. Coronal image with scale 0–140 %ID/g (a) and 0–3 %ID/g (b), arrows point at liver (L), kidneys (K), and tumor (T). Tumor volume was 0.15 cm^3



which manifested as increased tumor-to-normal organ ratios (Fig. 4). The more rapid wash-out of radioactivity from normal tissues could be explained by lower HER3 expression levels than in xenografts. We have previously observed such phenomena when studying tumor uptake of anti-HER2 Affibody molecules in xenografts with different HER2 expression levels [22]. Accordingly, a microSPECT imaging enabled visualization of LS174T xenografts at 4 h after injection, but there was also a noticeable uptake of radioactivity in the abdominal area. This elevated uptake in normal tissues might complicate interpretation of the images. However, we do not consider imaging of HER3 expression as the only imaging procedure. Most likely it would be used as complement to FDG-imaging to determine the HER3 status of already identified tumors for patient stratification to anti-HER3 therapy, similar to anti-HER2 imaging [23, 24].

Tumor-to-blood ratios for $^{99m}\text{Tc}(\text{CO})_3\text{-HEHEHE-Z}_{08699}$ were in the range of 6–7 at 4 h after injection. This is similar to peak-value ratios from good intact antibodies in murine models with HER2-expressing tumors at 2–3 days after injection [41]. It must be noted that for HER2-targeting antibodies, such values are obtained in models expressing 1.5–2 million receptors per cells, i.e., at least 60-fold higher than in our models, and in the absence of target expression in normal organs. Unfortunately, it is not possible to make a comparison with data for the targeting of HER3 using antibodies, as there is no successful imaging of HER3 in vivo using radiolabeled antibodies reported in the literature.

Targeting specificity to HER3 in vivo with $^{99m}\text{Tc}(\text{CO})_3\text{-HEHEHE-Z}_{08699}$ was evaluated using two different xenografts, BT474 (breast cancer) and LS174T (colorectal cancer). In both models (Fig. 5), co-injection of a large excess of non-

labeled Z_{08699} caused significant ($p < 0.05$) reduction in tumor uptake. This suggests a saturable uptake of $^{99m}\text{Tc}(\text{CO})_3\text{-HEHEHE-Z}_{08699}$ in the xenografts, and is evidence that tumor uptake of this imaging agent is HER3-specific. In addition, receptor saturation caused significant reduction of uptake in the salivary glands, lungs, liver, and stomach, i.e., organs expressing murine ErbB3. This demonstrates cross-species reactivity of $^{99m}\text{Tc}(\text{CO})_3\text{-HEHEHE-Z}_{08699}$ and validates that the murine model is relevant for the investigation of this agent. There was a significant difference between uptake in normal organs of mice bearing breast cancer xenografts, and mice bearing LS174T colorectal cancer xenografts in this study. In the latter case, the radioactivity concentration was significantly ($p < 0.05$) higher in blood, liver, spleen, and bone. It must be noted that the breast cancer model requires estradiol pellet implantations, which visibly influence the appearance and behavior of mice. It is likely that estradiol implantation alters the physiological processes rate in the animals, which might affect tracer biodistribution. There was no significant difference in the tumor uptake between models despite a 3-fold difference in receptor expression.

In conclusion, Affibody-based radionuclide imaging of HER3 expression in malignant tumors is feasible despite low expression in tumors and high expression in several tissues. Further work on optimizing labeling chemistry and tracer dosing is thus warranted.

Acknowledgments This work was supported by grants from the Swedish Cancer Society (Cancerfonden) and the Swedish Research Council (Vetenskapsrådet).

Conflict of interest The authors declare that they have no conflicts of interest.

References

- Yarden Y, Sliwkowski MX. Untangling the ErbB signalling network. *Nat Rev Mol Cell Biol.* 2001;2:127–37.
- Marmor MD, Skaria KB, Yarden Y. Signal transduction and oncogenesis by ErbB/HER receptors. *Int J Radiat Oncol Biol Phys.* 2004;58:903–13.
- Ocaña A, Pandiella A. Targeting HER receptors in cancer. *Curr Pharm Des.* 2013;19:808–17.
- Aurisicchio L, Marra E, Roscilli G, Mancini R, Ciliberto G. The promise of anti-ErbB3 monoclonals as new cancer therapeutics. *Oncotarget.* 2012;3:744–58.
- Hsieh AC, Moasser MM. Targeting HER proteins in cancer therapy and the role of the non-target HER3. *Br J Cancer.* 2007;97:453–7.
- Baselga J, Swain SM. Novel anticancer targets: revisiting ERBB2 and discovering ERBB3. *Nat Rev Cancer.* 2009;9:463–75.
- Garrett JT, Olivares MG, Rinehart C, Granja-Ingram ND, Sánchez V, Chakrabarty A, et al. Transcriptional and posttranslational up-regulation of HER3 (ErbB3) compensates for inhibition of the HER2 tyrosine kinase. *Proc Natl Acad Sci U S A.* 2011;108:5021–6.
- Kruser TJ, Wheeler DL. Mechanisms of resistance to HER family targeting antibodies. *Exp Cell Res.* 2010;316:1083–100.
- Servidei T, Riccardi A, Mozzetti S, Ferlini C, Riccardi R. Chemoresistant tumor cell lines display altered epidermal growth factor receptor and HER3 signaling and enhanced sensitivity to gefitinib. *Int J Cancer.* 2008;123:2939–49.
- Jathal MK, Chen L, Mudryj M, Ghosh PM. Targeting ErbB3: the New RTK(id) on the Prostate Cancer Block. *Immunol Endocr Metab Agents Med Chem.* 2011;11:131–49.
- Ocana A, Vera-Badillo F, Seruga B, Templeton A, Pandiella A, Amir E. HER3 overexpression and survival in solid tumors: a meta-analysis. *J Natl Cancer Inst.* 2013;105:266–73.
- Tolmachev V, Stone-Elander S, Orlova A. Radiolabelled receptor-tyrosine-kinase targeting drugs for patient stratification and monitoring of therapy response: prospects and pitfalls. *Lancet Oncol.* 2010;11:992–1000.
- van Dongen GA, Poot AJ, Vugts DJ. PET imaging with radiolabeled antibodies and tyrosine kinase inhibitors: immuno-PET and TKI-PET. *Tumour Biol.* 2012;33:607–15.
- van Dongen GA, Visser GW, Lub-de Hooge MN, de Vries EG, Perk LR. Immuno-PET: a navigator in monoclonal antibody development and applications. *Oncologist.* 2007;12:1379–89.
- Wester HJ, Kessler H. Molecular targeting with peptides or peptide-polymer conjugates: just a question of size? *J Nucl Med.* 2005;46:1940–5.
- Löfblom J, Feldwisch J, Tolmachev V, Carlsson J, Ståhl S, Frejd FY. Affibody molecules: engineered proteins for therapeutic, diagnostic and biotechnological applications. *FEBS Lett.* 2010;584:2670–80.
- Orlova A, Magnusson M, Eriksson TL, Nilsson M, Larsson B, Höidén-Guthenberg I, et al. Tumor imaging using a picomolar affinity HER2 binding affibody molecule. *Cancer Res.* 2006;66:4339–48.
- Tolmachev V, Rosik D, Wällberg H, Sjöberg A, Sandström M, Hansson M, et al. Imaging of EGFR expression in murine xenografts using site-specifically labelled anti-EGFR 111In-DOTA-Z EGFR: 2377 Affibody molecule: aspect of the injected tracer amount. *Eur J Nucl Med Mol Imaging.* 2010;37:613–22.
- Tolmachev V, Malmberg J, Hofström C, Abrahmsén L, Bergman T, Sjöberg A, et al. Imaging of IGF-1R in prostate cancer xenografts using the Affibody molecule 111In-DOTA-Z IGF1R:4551. *J Nucl Med.* 2012;53:146–53.
- Ahlgren S, Orlova A, Rosik D, Sandström M, Sjöberg A, Baastrup B, et al. Evaluation of Maleimide Derivative of DOTA for Site-Specific Labeling of Recombinant Affibody Molecules. *Bioconjug Chem.* 2008;19:235–43.
- Friedman M, Orlova A, Johansson E, Eriksson T, Höidén-Guthenberg I, Tolmachev V, et al. Directed evolution to low nanomolar affinity of an epidermal growth factor receptor 1-binding Affibody molecule. *J Mol Biol.* 2008;376:1388–402.
- Tolmachev V, Tran TA, Rosik D, Abrahmsén L, Sjöberg A, Orlova A. Tumor targeting using Affibody molecules: an interplay of a target expression level, affinity and binding site composition. *J Nucl Med.* 2012;53:953–60.
- Baum RP, Prasad V, Müller D, Schuchardt C, Orlova A, Wennborg A, et al. Molecular imaging of HER2-expressing malignant tumors in breast cancer patients using synthetic 111In- or 68Ga-labeled affibody molecules. *J Nucl Med.* 2010;51:892–7.
- Sörensen J, Sandberg D, Carlsson J, Sandström M, Wennborg A, Feldwisch J, Tolmachev V, Åström G, Lubberink M, Garske-Roman U, Lindman H. First-in-Human Molecular Imaging of HER2 Expression in Breast Cancer Metastases Using the 111In-ABY-025 Affibody Molecule. *J Nucl Med.* 2014, in press.
- Kronqvist N, Malm M, Göström L, Gunneriusson E, Nilsson M, Höidén Guthenberg I, et al. Combining phage and staphylococcal surface display for generation of ErbB3-specific Affibody molecules. *Protein Eng Des Sel.* 2011;24:385–96.
- Robinson MK, Hodge KM, Horak E, Sundberg AL, Russeva M, Shaller CC, et al. Targeting ErbB2 and ErbB3 with a bispecific single-chain Fv enhances targeting selectivity and induces a therapeutic effect in vitro. *Br J Cancer.* 2008;99:1415–25.
- Löfblom J. Bacterial display in combinatorial protein engineering. *Biotechnol J.* 2011;6:1115–29.
- Malm M, Kronqvist N, Lindberg H, Gudmundsdóttir L, Bass T, Frejd FY, et al. Inhibiting HER3-mediated tumor cell growth with Affibody molecules engineered to low picomolar affinity by position-directed error-prone PCR-like diversification. *PLoS One.* 2013;8:e62791.
- Tolmachev V, Hofström C, Malmberg J, Ahlgren S, Hosseinimehr SJ, Sandström M, et al. HEHEHE-tagged affibody molecule may be purified by IMAC, is conveniently labeled with [^{99m}Tc(CO)₃](+), and shows improved biodistribution with reduced hepatic radioactivity accumulation. *Bioconjug Chem.* 2010;21:2013–22.
- Hofström C, Altai M, Honarvar H, Strand J, Malmberg J, Hosseinimehr SJ, et al. HAHAAA, HEHEHE, HIIHHI or HKHKHK: influence of position and composition of histidine containing tags on biodistribution of [99mTc(CO)₃]-labeled affibody molecules. *J Med Chem.* 2013;56:4966–74.
- Waibel R, Alberto R, Willuda J, et al. Stable one-step technetium-99 m labeling of His-tagged recombinant proteins with a novel Tc(I)-carbonyl complex. *Nat Biotechnol.* 1999;17:897–901.
- Yoshioka T, Nishikawa Y, Ito R, Kawamata M, Doi Y, Yamamoto Y, et al. Significance of integrin αvβ5 and erbB3 in enhanced cell migration and liver metastasis of colon carcinomas stimulated by hepatocyte-derived heregulin. *Cancer Sci.* 2010;101:2011–8.
- Janmaat ML, Rodriguez JA, Jimeno J, Kruyt FA, Giaccone G. Kahalalide F induces necrosis-like cell death that involves depletion of ErbB3 and inhibition of Akt signaling. *Mol Pharmacol.* 2005;68:502–10.
- Kimura F, Iwaya K, Kawaguchi T, Kaise H, Yamada K, Mukai K, et al. Epidermal growth factor-dependent enhancement of invasiveness of squamous cell carcinoma of the breast. *Cancer Sci.* 2010;101:1133–40.
- Wällberg H, Orlova A. Slow internalization of anti-HER2 synthetic affibody monomer 111In-DOTA-ZHER2:342-pep2: implications for development of labeled tracers. *Cancer Biother Radiopharm.* 2008;23:435–42.
- Tolmachev V, Wällberg H, Sandström M, Hansson M, Wennborg A, Orlova A. Optimal specific radioactivity of anti-HER2 Affibody molecules enables discrimination between xenografts with high and low HER2 expression levels. *Eur J Nucl Med Mol Imaging.* 2011;38:531–9.
- Orlova A, Nilsson F, Wikman M, Widström C, Ståhl S, Carlsson J, et al. Comparative in vivo evaluation of technetium

- and iodine labels on an anti-HER2 Affibody for single-photon imaging of HER2 expression in tumors. *J Nucl Med.* 2006;47:512–9.
38. Orlova A, Tolmachev V, Pehrson R, Lindborg M, Tran T, Sandström M, et al. Synthetic Affibody Molecules: A Novel Class of Affinity Ligands for Molecular Imaging of HER2-Expressing Malignant Tumors. *Cancer Res.* 2007;67:2178–86.
39. Tolmachev V, Varasteh Z, Honarvar H, Eriksson O, Jonasson P, Frejd FY, Abrahmsen L, Orlova A. Imaging of PDGFR β expression in glioblastoma xenografts using Affibody molecule ¹¹¹In-DOTA-Z09591. *J Nucl Med.* 2014;55:294–300.
40. Orlova A, Hofström C, Strand J, Varasteh Z, Sandstrom M, Andersson K, et al. [^{99m}Tc(CO)₃]⁺-(HE)₃-ZIGF1R:4551, a new affibody conjugate for visualization of insulin-like growth factor I receptor expression in malignant tumours. *Eur J Nucl Med Mol Imaging.* 2013;40(3):439–49.
41. Tolmachev V. Imaging of HER-2 overexpression in tumors for guiding therapy. *Curr Pharm Des.* 2008;14:2999–3019.